Published in final edited form as:

Nat Med. 2008 November ; 14(11): 1236–1246. doi:10.1038/nm.1877.

Suppressed NFAT-dependent VEGFR1 expression and constitutive VEGFR2 signaling in infantile hemangioma

Masatoshi Jinnin[1], **Damian Medici**[1], **Lucy Park**[1], **Nisha Limaye**[2], **Yanqiu Liu**[1], **Elisa Boscolo**[3], **Joyce Bischoff**[3], **Miikka Vikkula**[2], **Eileen Boye**[1], and **Bjorn R. Olsen**[1]

[1] Department of Developmental Biology, Harvard School of Dental Medicine, 188 Longwood Avenue, Boston, MA 02115

[2] Human Molecular Genetics (GEHU), de Duve Institute, Universite Catholique de Louvain, Brussels, Belgium, B-1200

[3] Vascular Biology Program, Department of Surgery, Children's Hospital Boston, 300 Longwood Avenue, Boston, MA 02115

Abstract

Infantile hemangiomas are localized and rapidly growing regions of disorganized angiogenesis. We demonstrate that expression of VEGFR1 in hemangioma endothelial cells (hemEC) and tissue is only 10−20% of that in controls. Low VEGFR1 levels result in VEGF-dependent activation of VEGFR2 and downstream pathways. We show that *VEGFR1* transcription is NFAT-dependent, and that low VEGFR1 expression in hemEC is caused by reduced activity of a pathway involving β1 integrin, the integrin-like receptor TEM8, VEGFR2 and NFAT.

In a subset of individuals with hemangioma, we find missense mutations in *VEGFR2* or *TEM8*. Further studies indicate that the mutations result in increased interaction between VEGFR2, TEM8 and β1 integrin and inhibition of integrin activity. Normalization of the constitutive VEGFR2-signaling in hemEC with soluble VEGFR1 and antibodies that block VEGF or stimulate β1 integrin suggests that local administration of these or similar agents may be effective in hemangioma treatment.

Introduction

Infantile hemangiomas, localized lesions of disorganized angiogenesis, are the most common tumors of infancy (10% of Caucasian infants). They typically appear around the second week of life, proliferate over 6−10 months and involute over 7−10 years[1-3]. Endothelial cells within the lesions (hemEC) exhibit X-chromosome inactivation patterns of clonality, upregulated expression of some markers and downregulation of others[1,4-6]. This expression pattern is stably maintained in cultured hemEC, and it differs from that of other endothelial cells, including human dermal microvascular endothelial cells (HDMEC). It has

Corresponding authors: Bjorn R. Olsen and Eileen Boye Phone: 617−432−1874 Fax: 617−432−0638 bjorn_olsen@hms.harvard.edu, eileen_boye@hms.harvard.edu.

been proposed that hemEC are either differentiated toward the placental microvascular phenotype or originate from placental endothelial cells7,8. Additionally, epidemiological studies and rare familial cases suggest a genetic influence9,10.

We report here that cultured hemEC from nine unrelated individuals with hemangioma (Supplementary Table 1 online) share a phenotype of constitutively active vascular endothelial growth factor receptor 2 (VEGFR2) signaling. This is associated with low expression of vascular endothelial growth factor receptor 1 (VEGFR1), a receptor that is known to bind VEGF with high affinity, thereby preventing it from activating VEGFR2 and its downstream targets11,12.

In a candidate gene screen of these individuals for potential disease associated mutations, we find germline heterozygosity for missense mutations in the gene encoding the integrin-like receptor TEM813,14 in one individual and in *VEGFR2* in two others. Investigation of the impact of these mutations elucidates a pathway controlling *VEGFR1* transcription that involves TEM8, VEGFR2, β1 integrin and NFAT. Although the mutations in TEM8 or VEGFR2 inhibit the activity of this pathway, reduced NFAT activity and VEGFR1 expression are found in all nine hemEC.

Results

VEGFR2-dependent signal transduction is upregulated in hemEC

In initial experiments, we compared phosphorylation levels of VEGFR2 between HDMEC and hemEC primary cultures. Primary cells from nine individuals with hemangioma were carefully characterized and data on eight of these (all the females) were reported in a previous publication demonstrating clonality1 (Supplementary Table 1 online). Tyrosine phosphorylation of VEGFR2 at residue Tyr1175 was very low in lysates of HDMEC cultured without exogenous VEGF, but high in lysates from hemEC (Fig. 1a). Addition of VEGF-specific neutralizing antibodies to the cultures reduced levels of phospho-VEGFR2 (Fig. 1a). Using phospho-peptide arrays to assess kinase activities, hemEC lysates showed increased activity of kinases, reflected by increased phosphorylation of VEGFR2 peptides or of peptides representing multiple downstream targets. Phosphorylation patterns in hemEC were on average very similar to those of HDMEC treated with VEGF, consistent with activation of VEGFR2 signaling pathways (Table 1). Phosphorylation of peptides representing EGF and FGF receptors was at background levels for all lysates (Supplementary Table 2 online).

Quantitative measurement of VEGFR2 protein by ELISA showed that it was slightly reduced in hemEC compared to HDMEC (Supplementary Fig. 1 online). Quantitative multiplex assays confirmed high phosphorylation levels of VEGFR2 targets, ERK and Akt, in hemEC lysates (Fig. 1b) and demonstrated increased protein levels of several downstream targets of VEGFR2 signaling. For example, levels of endogenous VEGF and GLUT-1 were as high in unstimulated hemEC as in VEGF-stimulated HDMEC (Fig. 1b). Migratory and proliferative activities in hemEC were almost identical to activities of VEGF-stimulated HDMEC (Fig. 1c,d). Treatment with the soluble form of VEGFR1 (sR1) or *VEGFR2* silencing RNA (siRNA) (Supplementary Fig. 1 online) strongly inhibited these activities

(Fig. 1c,d). The results suggest that increased VEGFR2 phosphorylation depends on VEGF binding at the cell surface.

Decreased VEGFR1 expression caused by reduced NFAT activation in hemEC

Since addition of VEGF-specific antibody or sR1 protein to hemEC cultures reduced phosphorylation of VEGFR2 and downstream targets (Fig. 1a,b), we used ELISA to determine levels of the VEGF decoy receptor VEGFR1 in several types of control cells and in hemEC from all nine subjects with hemangioma. The results showed that VEGFR1 protein levels in hemEC were only 10−20% of those in control cells (Fig. 2a). Isoform-specific RT-PCR15 showed that transcripts encoding both membrane-bound VEGFR1 (mR1) and sR1 were reduced in hemEC compared to HDMEC (not shown). Stable overexpression of mR1 in hemEC reduced phospho-VEGFR2 and phospho-ERK levels (Fig. 2b). Overexpression of a kinase-dead mutant, mut mR116, had the same effect as mR1. Overexpression of a mutant VEGFR1 lacking the extracellular domain had no effect (not shown). Therefore, we conclude that the reduced expression of VEGFR1, combined with increased levels of endogenous VEGF (Fig. 1b), maintains increased VEGFR2 activation and signaling in hemEC.

Low VEGFR1 transcript and protein levels in all the hemECs led us to sequence 1 kb of the *VEGFR1* promoter in hemEC DNA from all nine subjects. Finding no sequence changes, we asked how *VEGFR1* is transcriptionally regulated in endothelial cells. We identified a potential NFAT binding site (GGACCCT) at −83 to −89, next to an AP-1 binding site, in a region of the *VEGFR1* promoter reported to contain a transcriptional activator site17. Replacing GGA (at −87 to −89) with TCA in a luciferase-containing reporter essentially eliminated luciferase activity in HDMEC (Fig. 2c). In contrast, replacing GGA with TCA at a site (−65 to −67) downstream of the AP-1 binding site, had no effect on activation of the reporter (not shown). A double-stranded oligonucleotide containing the wild-type GGA sequence at −87 to −89 had substantial binding activity for NFATc1 (not shown) and NFATc2 (Fig. 2c). In contrast, an oligonucleotide containing TCA had no NFAT binding activity. Overexpression of a constitutively active form of NFATc1 stimulated *VEGFR1* transcription in both HDMEC and hemEC (Supplementary Fig. 2 online).

NFAT is activated by the Ca^{++}- and calmodulin-dependent phosphatase calcineurin 18 and is a target of VEGFR2 signaling in endothelial cells. Surprisingly, not only were *VEGFR1* transcripts reduced in hemEC, but transcript levels of other known NFAT-regulated genes, *DSCR1 (MCIP1)*, *MCP-1* and *COX-2*19-21, were also significantly lower in hemEC than in HDMEC (Fig. 2d), indicating low basal NFAT activity in hemEC. No differences were found between transcript levels for *NFATc1* or *NFATc2* in HDMEC and hemEC (Fig. 2d). In addition, real-time PCR showed *COX-2/VEGFR2* and *VEGFR1/VEGFR2* transcript ratios to be considerably lower in proliferating hemangioma tissue and hemEC than in HDMEC and other control endothelial cells, control tissues and involuting hemangioma tissue (Fig. 2e). Incubation of HDMEC with a cell-permeable inhibitor of NFAT-calcineurin interaction decreased *VEGFR1* transcript levels and increased VEGFR2 and ERK phosphorylation in a dose-dependent manner (Fig. 2f), modeling the fact that NFAT inactivation is indeed associated with the hemangioma phenotype described above through VEGFR1 down-

regulation. A low level of NFAT activation in hemEC was supported by finding that antibody staining for NFATc2 showed significantly less nuclear staining in hemEC than in HDMEC after stimulation with VEGF or ionomycin (Supplementary Fig. 3a online). Preliminary experiments demonstrated that ionomycin-stimulated release of Ca^{++} from intracellular stores was reduced in hemEC compared to HDMEC (Supplementary Fig. 3b online).

Reduced β1 integrin activity in hemEC

To address the question of what may cause the suppression of the NFAT-VEGFR1 pathway in hemEC, we examined the activation state of their integrin receptors. A link between integrins and Ca^{++} signaling is well established. For example, treatment with integrin-specific stimulatory antibody increases Ca^{++} levels in endothelial cells22-24, and integrin-mediated cell adhesion can trigger calcium influx25,26.

A connection between integrin and NFAT is supported by the following results: Treatment of HDMEC or hemEC with β1 integrin-specific stimulatory antibody increased association of NFATc2 with the *VEGFR1* promoter in chromatin immunoprecipitates (Fig. 3a) and induced an increase in the transcript levels of *VEGFR1* and *COX-2* in both HDMEC and hemEC (Fig. 3b). In hemEC, the antibody-stimulated increase in VEGFR1 expression reduced VEGFR2 phosphorylation (Supplementary Fig. 4 online). Treatment of HDMEC with siRNA for *NFATc2* blocked the stimulatory effect on *VEGFR1* expression (see below Fig. 5c).

Therefore, we compared integrin functions in HDMEC and hemEC. Staining of cell cultures with antibody to total β1 integrin showed no difference (Fig. 3c). However, immunostaining with an antibody (HUTS-21) that recognizes only active β1 integrin27, showed significantly decreased reactivity at the cell surface of hemEC compared with HDMEC (Fig. 3c). Consistent with decreased β1 integrin activity on the surface of hemEC we found that adhesion of hemEC to type I collagen or fibronectin was significantly lower than that of HDMEC, but no differences were seen on vitronectin (Supplementary Fig. 5 online).

Moreover, when suspended cells were incubated without fibronectin, the difference in expression levels of NFAT-regulated genes (*VEGFR1* and *COX-2*) were minimal; in the presence of fibronectin the levels were increased in HDMEC, but not in hemEC (not shown). Finally, phosphorylation of Tyr397 in focal adhesion kinase, an indicator of integrin activation28-30, was significantly reduced in all the nine hemECs compared to HDMEC and HUVEC (not shown).

TEM8 and VEGFR2 mutations and their effect on VEGFR1 expression

In light of the evidence9,10,31 for a genetic component to hemangioma formation, we asked whether suppressed NFAT activation and low VEGFR1 expression in hemEC could result from germline or somatic mutations. Using a targeted candidate gene approach, we sequenced the complete coding sequences of 24 selected genes using DNA from the nine hemEC cultures and confirmed specific results with DNA from blood of the relevant subjects. In addition to neutral and common polymorphisms, we found heterozygosity for

nucleotide changes resulting in potential disease-associated amino acid substitutions in three of the nine individuals with hemangioma (Supplementary Tables 1 and 3 online).

A germline G-to-A transition replaces alanine with threonine in the transmembrane domain of the integrin-like molecule TEM8 in hemEC4 (referred to as hemEC4$^{(TEM8)}$ below) (Fig. 4a). Using allele-specific PCR, we screened for the A allele in blood genomic DNA samples collected from 110 individuals with a history of hemangioma and 295 “controls” (all Caucasian; see below). No other individual carrying the A allele was found.

TEM8 is expressed as three alternatively spliced transcripts (variants 1, 2 and 3)13 (Fig. 4a). Stable retroviral overexpression of HA-tagged wild-type TEM8 in HDMEC stimulated VEGFR1 expression (Fig. 4b) without changing the low levels of phospho-VEGFR2 and phospho-ERK. Overexpression of HA-tagged mutant TEM8 or variant 3 (lacking the cytoplasmic and transmembrane domains) reduced VEGFR1 expression and increased phospho-VEGFR2 and phospho-ERK levels. Overexpression of wild-type TEM8 in hemEC2 and 21A as well as hemEC4$^{(TEM8)}$ increased VEGFR1 expression and reduced phospho-VEGFR2 and phospho-ERK levels (Fig. 4c).

A T-to-C germline transition replaces cysteine by arginine at position 482 in the Ig-like domain V of the VEGFR2 extracellular region in hemEC2 and 17B (referred to as hemEC2$^{(VEGFR2)}$ and hemEC17B$^{(VEGFR2)}$ below) (Fig. 4d). Allele-specific PCR identified heterozygosity for the same change in 8 blood genomic DNA samples collected from an additional 105 individuals with a history of hemangioma (10 total out of 114 individuals) and in 12 DNA samples from 295 “controls” (all Caucasian). The controls include individuals with hemangioma at the population frequency (10%) (see **Methods**). On that basis, the difference in the frequency of the C482R change among individuals with a history of hemangioma and controls is statistically significant ($P = 0.02$, Fisher's exact two-tailed test). No difference in receptor expression and VEGF-induced phosphorylation was apparent between wild-type and C482R mutant receptor transiently expressed in 293-EBNA cells (see below), probably because the mutation is located outside the VEGF-binding region32.

Retroviral overexpression of His-tagged wild-type VEGFR2 in HDMEC resulted in increased VEGFR1 expression, but no significant changes in phospho-VEGFR2 and phospho-ERK levels (Fig. 4e). Unlike mutant TEM8, overexpression of His-tagged mutant (C482R) VEGFR2 in HDMEC reduced VEGFR1 expression only slightly (Fig. 4e). Overexpression of wild-type VEGFR2 in hemEC4$^{(TEM8)}$ and 21A as well as hemEC2$^{(VEGFR2)}$ and hemEC17B$^{(VEGFR2)}$ increased VEGFR1 expression and reduced levels of phospho-VEGFR2 and phospho-ERK (Fig. 4f). To address the question of whether this stimulatory effect requires signaling through the VEGFR2 kinase domain, we transfected various VEGFR2 expression constructs into hemEC. Truncating the cytoplasmic domain or replacing three of the tyrosine residues within the cytoplasmic domain with phenylalanines did not compromise the ability of VEGFR2 to stimulate VEGFR1 expression. Mutating the Cys482 codon to a serine codon did not affect the ability of VEGFR2 to stimulate VEGFR1 expression (Fig. 4g). Finally, a Q472H substitution, reported as a potential hemangioma mutation in VEGFR24, did not affect stimulation of VEGFR1 expression. We conclude, therefore, that the effect seen with the C482R mutation

on VEGFR1 expression is specific to that particular amino acid substitution. Taken together, the results further indicate that sequences within the extracellular Ig-like domain V of VEGFR2 are critical for the ability of VEGFR2 to stimulate VEGFR1 expression.

Abnormal interaction between VEGFR2, TEM8 and β1 integrin

The levels of β1 integrin and TEM8 were almost the same in lysates of hemEC and control cells. However, immune complexes from hemEC extracts generated with antibody to VEGFR2 contained substantially higher amounts of β1 integrin and TEM8 than complexes from HDMEC or HUVEC extracts (Fig. 5a). Similar results were obtained in reciprocal immunoprecipitation assays with antibody to TEM8 (not shown).

To determine whether the (C482R) VEGFR2 and (A326T) TEM8 mutations affect the recruitment of the proteins into immune complexes with β1 integrin, we expressed mutant and wild-type receptors in 293-EBNA cells, since these cells express β1 integrin but neither VEGFR2 nor TEM814,33-35. Western blotting of immunoprecipitates generated with antibody to VEGFR2 showed that the mutations enhanced recruitment of the proteins into a complex with β1 integrin (Fig. 5b), suggesting that they increase the affinity of VEGFR2 and TEM8 for each other, β1 integrin or another common partner within the complex. Similar results were obtained in reciprocal immunoprecipitation assays with antibody to TEM8 (not shown).

Treatment of HDMEC with siRNA for *TEM8*, *VEGFR2* or *NFATc2* blocked the stimulatory effect on *VEGFR1* expression by β1 integrin-specific stimulatory antibody or VEGF (Fig. 5c). The data indicate that TEM8, VEGFR2 and β1 integrin functionally interact to control *VEGFR1* expression in an NFAT-dependent manner in endothelial cells. This interaction, and consequently regulation of VEGFR1 expression, is compromised in hemEC.

Next, we examined the effects of expressing A326T mutant TEM8 or C482R mutant VEGFR2 on activation of NFAT and β1 integrin, proliferation and migration in HDMEC. Expression of mutant TEM8 significantly reduced association of NFATc2 with the VEGFR1 promoter; expression of wild-type TEM8 or wild-type VEGFR2 in hemEC4$^{(TEM8)}$ increased the association (Fig. 5d). Overexpression of mutant TEM8 in HDMEC significantly reduced the amount of active β1 integrin as assessed by staining with HUTS-21 antibody (Fig. 3c). In contrast, overexpression of mutant VEGFR2 reduced the amount of active β1 integrin only slightly (Fig. 4e). Overexpression of wild-type VEGFR2 or TEM8 in hemEC increased HUTS-21 staining (Fig. 3c). Finally, stably overexpressing mutant TEM8 in HDMEC stimulated BrdU incorporation and migration to levels approaching those of hemEC4$^{(TEM8)}$ (Fig. 5e). These results correlate well with changes in VEGFR1 levels in HDMEC or hemEC transfected with wild-type or mutant TEM8 or mutant VEGFR2 (Fig. 4).

Discussion

We demonstrate that *VEGFR1* is an NFAT target gene in endothelial cells and that all nine hemEC studied here show downregulation of NFAT targets (Fig. 5f). As a consequence of reduced VEGFR1 decoy function, VEGFR2 and its downstream targets are activated/phosphorylated in a VEGF-dependent manner and the protein levels of downstream targets,

such as VEGF and GLUT-1, are increased. Proliferation and migration of hemEC are also upregulated. In addition, reduced NFAT activation in hem EC is associated with low activity of β1 integrin. Finally, we find increased interaction between β1 integrin, the integrin-like receptor TEM8 and VEGFR2 in all nine hemEC. The only differences we have found between the nine hemEC are the missense changes in TEM8 and VEGFR2 in three of the nine hemEC. Both mutations have a dramatic effect on the amount of TEM8 and β1 integrin in immune complexes with VEGFR2 when the proteins are expressed in 293 cells, similar to what is seen with lysates from all hemECs. On this basis we suggest that the hemEC phenotype of low "setpoint" of integrin-NFAT activation is a consequence of the formation of an abnormal complex between VEGFR2, TEM8 and β1 integrin (Fig. 5f).

In hemEC, increased complex formation is associated with reduced level of active β1 integrin at the cell surface, suggesting that β1 integrin (and possibly other integrins) are in the closed, low-affinity conformation or somehow blocked in hemEC. Thus, the phenotype of repressed integrin-NFAT activation and VEGFR1 expression in hemEC2$^{(VEGFR2)}$, hemEC4$^{(TEM8)}$ and hemEC17B$^{(VEGFR2)}$ may be caused by inhibition of integrin activation within the TEM8/VEGFR2-containing complex. Determining the detailed mechanistic steps in the integrin-NFAT pathway will require further studies. However, based on what is currently known about NFAT activation mechanisms such studies may address integrin control of processes related to dephosphorylation of inactive NFAT in the cytoplasm and the control of nuclear import of the transcription factor.

Although all hemEC share a common phenotype, we have not found mutations among the candidate genes sequenced so far in the other six hemEC (e.g. 21A). However, overexpression of wild-type VEGFR2 or TEM8 normalizes the phenotype even in EC21A. This suggests that hemangioma formation in the six patients for which we have not yet found mutations may be associated with mutations in genes encoding other pathway components, upstream of NFAT, perhaps other cell surface or cytoplasmic proteins that interact with integrins, TEM8 or VEGFR2. Thus, identifying other components of the complex may provide good candidates for future mutation screens.

In the mechanistic model proposed here for hemangioma endothelial dysfunction, both VEGFR2 and TEM8 mutations have dominant inhibitory effects on integrin-NFAT activation. However, the two mutations differ in their ability to induce the hemEC phenotype when the mutant proteins are stably expressed in control HDMEC. Overexpression of mutant TEM8 in HDMEC reduces active β1 integrin on the cell surface, decreases the association between NFAT and the VEGFR1 promoter, and decreases VEGFR1 expression. The similarity between the consequences of overexpressing mutant TEM8 (A326T) and variant 3 (lacking the transmembrane and cytoplasmic domains) in HDMEC suggests that the cytoplasmic domain of TEM8 is required for its ability to positively control integrin-NFAT activation and VEGFR1 expression, and that many types of mutations, even in introns, in *TEM8* could have similar effects. Therefore, sequencing of the entire *TEM8* gene (including introns) in additional hemangioma DNA samples may be illuminating.

Overexpression of the C482R mutant VEGFR2 in HDMEC decreases VEGFR1 expression and staining with the HUTS-21 antibody only slightly. However, overexpression of wild-type VEGFR2 in hemEC normalizes the amount of active integrin detected with the HUTS-21 antibody, increases the association between NFATc2 and the *VEGFR1* promoter, and increases VEGFR1 expression. This indicates that there is a critical difference between wild-type and C482R mutant VEGFR2 proteins in their ability to stimulate VEGFR1 expression. Further work will be needed to determine whether these different effects of the TEM8 and VEGFR2 mutations are caused by differences in the relative amounts of TEM8 and VEGFR2 proteins in HDMEC or reflect differences in the "strength" of the mutations. It is also possible that polymorphisms in other genes may contribute to the pathogenetic process in hemEC from individuals who carry the relatively common C482R missense change in the extracellular domain of VEGFR2.

Considering all these data together, we conclude that the TEM8 and VEGFR2 amino acid sequence changes represent risk factor mutations for infantile hemangioma. Both receptors are co-expressed with the endothelial marker CD31 in hemangioma tissue (not shown) and both sequence changes affect highly conserved amino acid residues. These heterozygous germline missense changes in *VEGFR2* and *TEM8* do not appear to cause significant systemic vascular abnormality in the individuals who carry them. In that sense, they are similar to germline mutations in other genes that cause localized vascular lesions. Venous or glomuvenous malformations are caused by a combination of germline and somatic mutations in *TIE2* or *glomulin*, respectively36,37. Since all the nine different hemEC we have analyzed in this study exhibit clonality1, the germline mutations in hemEC2$^{(VEGFR2)}$, hemEC4$^{(TEM8)}$ and hemEC17B$^{(VEGFR2)}$ must be associated with a secondary somatic event to trigger the expansion of endothelial cells within the lesions. To account for the difference in progression between hemangioma (which undergoes age-dependent involution) and venous or glomuvenous malformations (which do not) we speculate that this secondary lesion-triggering event in an individual carrying a germline risk mutation for hemangioma may be a physiological event (e.g. emboli of placental cells or perinatal hypoxia38,39) rather than a somatic mutation.

Several types of data support the view that the signaling phenotype of cultured hemEC is similar to that of endothelial cells within the tumors. First, *VEGFR1/VEGFR2* and *COX-2/VEGFR2* transcript ratios are as low in proliferating hemangioma as in cultured hemEC compared with control tissues and involuting hemangioma. Second, increased GLUT-1 and VEGF expression in hemEC is consistent with reports of increased GLUT-1 and VEGF in hemangioma tissue5,40. Third, increased proliferation of hemEC *in vitro* matches increased proliferation *in vivo*41. Therefore, our data suggest that locally administered anti-VEGF therapy or agents targeting other components of the signaling pathway could be effective in treating rapidly growing hemangiomas.

Methods

Sections on Antibodies, Immunoblotting and immunoprecipitation, DNA affinity precipitation assay, Quantitative real-time Polymerase Chain Reaction (PCR), Mutation detection, sequencing and allele specific PCR, Transfection and reporter assays,

Immunocytochemistry and **Cell adhesion assays** are presented in Supplementary Methods online.

Plasmids

The constitutive active form of NFATc1 was previously described37. The construct containing the *VEGFR1* promoter linked to luciferase was as described42. Full-length human *VEGFR1* cDNA was inserted in a pcDNA3.1 vector 43. Full-length human *VEGFR2* cDNA in pcDNA3.1/Myc-His(+)B and human cDNA in pcDNA3 encodingVEGFR1 with Y1213F mutation were previously published16,44. His epitope tagging of VEGFR2 was done by PCR. Full-length human cDNAs encoding TEM8 with HA-tag or TEM8 variant 3 and cloned into pIREShyg2 were as described45. The cDNA fragments were amplified by PCR and cloned into the bicistronic retroviral vector pMXs46. Point mutations were introduced using the QuickChange site-directed mutagenesis kit (Stratagene) and verified by sequencing.

Isolation of endothelial cells, cell culture and patient material

Primary cultures of hemEC were established from nine Caucasian patients; all females, except one (no. 2). All, except two (no. 17 and no. 21), had single lesions (Supplementary Table 1 online). These hemEC were selected for the studies because they are derived from typical proliferating hemangioma6, exhibit clonality1 and cryopreserved cells at low population doublings (3−5) are available. All properties we have examined have remained constant over several generations (5−15) in culture.

Age-matched neonatal foreskin-derived HDMEC and normal human female skin endothelial cells (HFSEC) isolated from face of age-matched female infants were obtained using identical methods described by Boye *et al*1. Cord blood endothelial progenitor cells (cbEPC) were isolated as described by Kahn *et al*47. Briefly, in the case of HDMEC, HFSEC and hemEC, tissue samples were digested with trypsin, the cells were resuspended in EBM-A as described 1 and grown to preconfluence. The ECs were purified from such primary cultures using *Ulex europaeus* I lectin-coated magnetic beads1. In case of cbEPC, mononuclear cells were isolated by Ficoll-Hypaque density gradient sedimentation, plated in enriched EBM-2 medium and selected using *Ulex europaeus* I lectin- or CD31-coated magnetic beads47. Human umbilical vein endothelial cells (HUVEC) were purchased from Clonetics. All HDMEC cultures were tested for the presence of transcripts of the lymphatic endothelial marker *PROX1* by PCR and shown to be negative.

All the different endothelial cell types were grown in EGM-2 (Clonetics) on AF-coated dishes (Cascade Biologics), with 20% heat-inactivated fetal bovine serum (FBS) (Hyclone), 1x Antibiotic-antimycotic (GIBCO-BRL) in 5% CO_2 at 37 °C. 293-EBNA (Invitrogen) cells were grown following the manufacturer's recommendation. Prior to specific experiments, endothelial and 293-EBNA cells were cultured in the absence of serum and supplemental growth factors for 12−24 hours.

Six resected infantile hemangioma specimens (hem75, hem76, hem82, I-39, I-47 and I-52) were obtained for extraction of RNA. Tissues from full-term placenta and foreskin were

obtained as described previously48. Blood-derived genomic DNA was extracted from 105 unrelated Caucasian individuals with hemangioma and 295 controls using the Puregene DNA purification kit (Gentra Systems). These control individuals likely include hemangioma at the population frequency (10%) since it is practically impossible to find individuals with a documented absence of hemangioma in early childhood. Collection and handling of all human material was according to guidelines of Harvard Medical School Committee on Human Studies and the Children's Hospital Boston, Committee on Clinical Investigation (CHB CCI) for protection of research subjects and informed consent was obtained from all subjects.

Chromatin immunoprecipitation

The interaction of NFATc2 with the *VEGFR1* promoter *in vivo* was analyzed using ChIP-IT (Active Motif) according to the methods recommended by the manufacturer. Cellular DNA was sheared using an Enzymatic Shearing Cocktail for 10 min. The chromatin (input DNA) was immunoprecipitated with 5 μg of NFATc2-specific antibody (Santa Cruz) or an isotype control mouse IgG. DNA purified from immunoprecipitates was amplified by PCR using human *VEGFR1* promoter-specific primers: 5'-CTGGGAGGAAGAAGAGGGTAGGTG-3' and 5'-CGAGGGCGGGGGCGATTTAT-3'. These primers amplify a 124 bp fragment containing the putative NFAT site of interest. PCR conditions were as follows: 95 °C for 15 min, followed by denaturation for 30 s at 95 °C, annealing for 30 s at 60 °C, extension for 30 s at 72 °C. The amplified DNA products were analyzed by quantitative real-time PCR as described above or resolved by agarose gel electrophoresis.

Quantitative protein analysis

Levels of VEGF receptors were measured with a specific ELISA kit (R&D Systems). Quantitative multiplex ELISA was performed using the Beadlyte Universal Signaling Kit and protocol (Upstate Biotechnology). Antibodies used for bead conjugation were specific for VEGF, GLUT-1, VEGFR2, phospho-Akt, and α-tubulin. Ten μg of each antibody was conjugated to carboxylated beads using Bioplex Amine Coupling Kit and protocol (Bio-Rad Laboratories). The 8-plex Cell Signaling Kit (Upstate Biotechnology) was used to assess phospho-ERK1/2. Samples were analyzed using a Luminex 200 multiplex station. Five hundred beads were isolated for each protein. Data were normalized by dividing experimental values by control (α-tubulin) values.

Kinase arrays

Arrays containing 144 kinase substrate probes were provided by PamGene International B.V. (http://www.pamgene.com) and used following their protocol. Briefly, chips were incubated with cellular extracts in the presence of ATP and a fluorescently labeled antibody (PY20) to phospho-tyrosine for real-time detection of phospho-tyrosine residues using a PamStation 4. Data analysis used Bionavigator software (PamGene).

Proliferation and migration assay

BrdU labelling for flow cytometry was done using a kit (Roche). Cells were analysed in a flow cytometer at 488nm. Migration was assessed using the Innocyte Cell Migration Assay

Kit (EMD Biosciences). Cells migrated towards 10% serum with 25 ng ml^{-1} exogenous VEGF into the lower chambers of 96-well transwell plates containing 8 μm pores. Migrated cells were stained with Calcein-AM fluorescent dye. Excitation max (485 nm)/emission max (520 nm) was assessed using a fluorescent plate reader (BD FACSArray bioanalyzer, BD Biosciences).

Statistical analysis

Mann-Whitney test for comparison of means, one-way analysis of variance (ANOVA) or two-tailed paired student's t test using GraphPad Prizm 4 software were used. Fisher's exact test was used for the *VEGFR2* allele-specific PCR results. *P* values less than 0.05 were considered significant.

Supplementary Material

Refer to Web version on PubMed Central for supplementary material.

Acknowledgments

Supported by the John B. Mulliken Foundation and Grants AR36820 and AR48564 from the US National Institutes of Health (to B.R.O.). We are indebted to Drs. J. B. Mulliken and L. Boon for providing essential surgical material for these studies. We thank N. A. Clipstone, M. Kurabayashi, S. Dias, L. Claesson-Welsh, S. Liu, and T. Kitamura for providing the constitutive active form of NFATc1, promoter construct for *VEGFR1*, expression vectors for *VEGFR1*, *VEGFR2* and mutant *VEGFR1*, *TEM8*, and pMXs vector, respectively. We thank R. Ruijtenbeek and R. Houtman for providing kinase arrays with reagents and equipment to run them; F. Naji and M. Dankers for kinase array bioinformatics assistance; T. Rector for assistance with protein multiplexing; J. Eastcott and J. Wylie-Sears for flow cytometry and technical assistance; S. Feske for NFATc2 antibody (clone 67.1) and advice; W. Kuo for technical advice. We thank Y. Pittel, S. Plotkina, N. Liu, A. Heilmann, Y. Ishida, Y. Yamamura for technical assistance and D. Glotzer for comments and advice on the manuscript.

References

1. Boye E, et al. Clonality and altered behavior of endothelial cells from hemangiomas. J. Clin. Invest. 2001; 107:745–752. [PubMed: 11254674]
2. Mulliken, J.; Young, A. Vascular Birthmarks: Hemangiomas and Malformations. W. B. Saunders Company; Philadelphia: 1988.
3. Mulliken JB. Cutaneous vascular anomalies. Semin. Vasc. Surg. 1993; 6:204–218. [PubMed: 8305975]
4. Walter JW, et al. Somatic mutation of vascular endothelial growth factor receptors in juvenile hemangioma. Genes Chrom. Cancer. 2002; 33:295–303. [PubMed: 11807987]
5. North PE, Waner M, Mizeracki A, Mihm MC Jr. GLUT1: a newly discovered immunohistochemical marker for juvenile hemangiomas. Hum. Pathol. 2000; 31:11–22. [PubMed: 10665907]
6. Li Q, Yu Y, Bischoff J, Mulliken JB, Olsen BR. Differential expression of CD146 in tissues and endothelial cells derived from infantile hemangiomas and normal human skin. J. Pathol. 2003; 201:296–302. [PubMed: 14517847]
7. Barnes CM, et al. Evidence by molecular profiling for a placental origin of infantile hemangioma. Proc. Natl. Acad. Sci. U S A. 2005; 102:19097–19102. [PubMed: 16365311]
8. North PE, et al. A Unique Microvascular Phenotype Shared by Juvenile Hemangiomas and Human Placenta. Arch. Dermatol. 2001; 137:559–570. [PubMed: 11346333]
9. Chiller KG, Passaro D, Frieden IJ. Hemangiomas of infancy: clinical characteristics, morphologic subtypes, and their relationship to race, ethnicity, and sex. Arch. Dermatol. 2002; 138:1567–1576. [PubMed: 12472344]

10. Haggstrom AN, et al. Prospective study of infantile hemangiomas: demographic, prenatal, and perinatal characteristics. J. Pediatr. 2007; 150:291–294. [PubMed: 17307549]
11. Ferrara N. The role of VEGF in the regulation of physiological and pathological angiogenesis. Exs. 2005:209–231. [PubMed: 15617481]
12. Roberts DM, et al. The vascular endothelial growth factor (VEGF) receptor Flt-1 (VEGFR-1) modulates Flk-1 (VEGFR-2) signaling during blood vessel formation. Am. J. Pathol. 2004; 164:1531–1535. [PubMed: 15111299]
13. Bradley KA, Mogridge J, Mourez M, Collier RJ, Young JA. Identification of the cellular receptor for anthrax toxin. Nature. 2001; 414:225–229. [PubMed: 11700562]
14. Werner E, Kowalczyk AP, Faundez V. Anthrax toxin receptor 1/tumor endothelium marker 8 mediates cell spreading by coupling extracellular ligands to the actin cytoskeleton. J. Biol. Chem. 2006; 281:23227–23236. [PubMed: 16762926]
15. Inoue T, et al. Identification of a vascular endothelial growth factor (VEGF) antagonist, sFlt-1, from a human hematopoietic cell line NALM-16. FEBS Lett. 2000; 469:14–18. [PubMed: 10708747]
16. Ito N, Huang K, Claesson-Welsh L. Signal transduction by VEGF receptor-1 wild type and mutant proteins. Cell Signal. 2001; 13:849–854. [PubMed: 11583921]
17. Wakiya K, Begue A, Stehelin D, Shibuya M. A cAMP response element and an Ets motif are involved in the transcriptional regulation of flt-1 tyrosine kinase (vascular endothelial growth factor receptor 1) gene. J. Biol. Chem. 1996; 271:30823–30828. [PubMed: 8940064]
18. Hogan PG, Chen L, Nardone J, Rao A. Transcriptional regulation by calcium, calcineurin, and NFAT. Genes Dev. 2003; 17:2205–2232. [PubMed: 12975316]
19. Hesser BA, et al. Down syndrome critical region protein 1 (DSCR1), a novel VEGF target gene that regulates expression of inflammatory markers on activated endothelial cells. Blood. 2004; 104:149–158. [PubMed: 15016650]
20. Hernandez GL, et al. Selective inhibition of vascular endothelial growth factor-mediated angiogenesis by cyclosporin A: roles of the nuclear factor of activated T cells and cyclooxygenase 2. J. Exp. Med. 2001; 193:607–620. [PubMed: 11238591]
21. Satonaka H, et al. Calcineurin promotes the expression of monocyte chemoattractant protein-1 in vascular myocytes and mediates vascular inflammation. Circ. Res. 2004; 94:693–700. [PubMed: 14739159]
22. Schwartz MA. Spreading of human endothelial cells on fibronectin or vitronectin triggers elevation of intracellular free calcium. J. Cell. Biol. 1993; 120:1003–1010. [PubMed: 7679387]
23. Leavesley DI, Schwartz MA, Rosenfeld M, Cheresh DA. Integrin beta 1- and beta 3-mediated endothelial cell migration is triggered through distinct signaling mechanisms. J. Cell. Biol. 1993; 121:163–170. [PubMed: 7681432]
24. Jones NP, Peak J, Brader S, Eccles SA, Katan M. PLCgamma1 is essential for early events in integrin signalling required for cell motility. J. Cell. Sci. 2005; 118:2695–2706. [PubMed: 15944397]
25. Aplin AE, Howe A, Alahari SK, Juliano RL. Signal transduction and signal modulation by cell adhesion receptors: the role of integrins, cadherins, immunoglobulin-cell adhesion molecules, and selectins. Pharmacol. Rev. 1998; 50:197–263. [PubMed: 9647866]
26. Sjaastad MD, Nelson WJ. Integrin-mediated calcium signaling and regulation of cell adhesion by intracellular calcium. Bioessays. 1997; 19:47–55. [PubMed: 9008416]
27. Luque A, et al. Activated conformations of very late activation integrins detected by a group of antibodies (HUTS) specific for a novel regulatory region (355−425) of the common beta 1 chain. J. Biol. Chem. 1996; 271:11067–11075. [PubMed: 8626649]
28. Schaller MD, Parsons JT. Focal adhesion kinase and associated proteins. Cur Opin Cell Biol. 1994; 6:705–710. [Review].
29. Guan J-L, Shalloway D. Regulation of focal adhesion-associated protein tyrosine kinase by both cellular adhesion and oncogenic transformation. Nature. 1992; 358:690–692. [PubMed: 1379699]
30. Abu-Ghazaleh R, Kabir J, Jia H, Lobo M, Zachary I. Src mediates stimulation by vascular endothelial growth factor of the phosphorylation of focal adhesion kinase at tyrosine 861, and

migration and anti-apoptosis in endothelial cells. Biochem. J. 2001; 360:255–264. [PubMed: 11696015]

31. Blei F, Walter J, Orlow SJ, Marchuk DA. Familial segregation of hemangiomas and vascular malformations as an autosomal dominant trait. Arch. Derm. 1998; 134:718–722. [see comments]. [erratum appears in Arch Dermatol 1998 Nov;134(11):1425]. [PubMed: 9645641]
32. Shinkai A, et al. Mapping of the sites involved in ligand association and dissociation at the extracellular domain of the kinase insert domain-containing receptor for vascular endothelial growth factor. J. Biol. Chem. 1998; 273:31283–31288. [PubMed: 9813036]
33. Kuriyama M, et al. Activation and translocation of PKCdelta is necessary for VEGF-induced ERK activation through KDR in HEK293T cells. Biochem. Biophys. Res. Commun. 2004; 325:843–851. [PubMed: 15541367]
34. Sun Y, et al. The kinase insert domain-containing receptor is an angiogenesis-associated antigen recognized by human cytotoxic T lymphocytes. Blood. 2006; 107:1476–1483. [PubMed: 16234362]
35. Shenoy PS, et al. beta1 Integrin-extracellular matrix protein interaction modulates the migratory response to chemokine stimulation. Biochem. Cell. Biol. 2001; 79:399–407. [PubMed: 11527209]
36. Vikkula M, et al. Vascular dysmorphogenesis caused by an activating mutation in the receptor tyrosine kinase TIE2. Cell. 1996; 87:1181–1190. [PubMed: 8980225]
37. Brouillard P, et al. Four common glomulin mutations cause two thirds of glomuvenous malformations ("familial glomangiomas"): evidence for a founder effect. J. Med. Genet. 2005; 42:e13. [PubMed: 15689436]
38. North PE, Waner M, Buckmiller L, James CA, Mihm MC Jr. Vascular tumors of infancy and childhood: beyond capillary hemangioma. Cardiovasc. Pathol. 2006; 15:303–317. [PubMed: 17113009]
39. Ritter MR, Reinisch J, Friedlander SF, Friedlander M. Myeloid cells in infantile hemangioma. Am. J. Pathol. 2006; 168:621–628. [PubMed: 16436675]
40. Takahashi K, et al. Cellular markers that distinguish the phases of hemangioma during infancy and childhood. J. Clin. Invest. 1994; 93:2357–2364. [PubMed: 7911127]
41. Razon MJ, Kräling BM, Mulliken JB, Bischoff J. Increased apoptosis coincides with onset of involution in infantile hemangioma. Microcirculation. 1998; 5:189–195. [PubMed: 9789259]
42. Akuzawa N, Kurabayashi M, Ohyama Y, Arai M, Nagai R. Zinc finger transcription factor Egr-1 activates Flt-1 gene expression in THP-1 cells on induction for macrophage differentiation. Arterioscler. Thromb. Vasc. Biol. 2000; 20:377–384. [PubMed: 10669633]
43. Fragoso R, et al. VEGFR-1 (FLT-1) activation modulates acute lymphoblastic leukemia localization and survival within the bone marrow, determining the onset of extramedullary disease. Blood. 2006; 107:1608–1616. [PubMed: 16249383]
44. Claesson-Welsh L. Signal transduction by vascular endothelial growth factor receptors. Biochem. Soc. Trans. 2003; 31:20–24. [PubMed: 12546646]
45. Liu S, Leppla SH. Cell surface tumor endothelium marker 8 cytoplasmic tail-independent anthrax toxin binding, proteolytic processing, oligomer formation, and internalization. J. Biol. Chem. 2003; 278:5227–5234. [PubMed: 12468536]
46. Kitamura T, et al. Retrovirus-mediated gene transfer and expression cloning: powerful tools in functional genomics. Exp. Hematol. 2003; 31:1007–1014. [PubMed: 14585362]
47. Khan ZA, et al. Endothelial progenitor cells from infantile hemangioma and umbilical cord blood display unique cellular responses to endostatin. Blood. 2006; 108:915–921. [PubMed: 16861344]
48. Picard A, et al. IFG-2 and FLT-1/VEGF-R1 mRNA levels reveal distinctions and similarities between congenital and common infantile hemangioma. Ped. Res. 2008; 63:263–267.

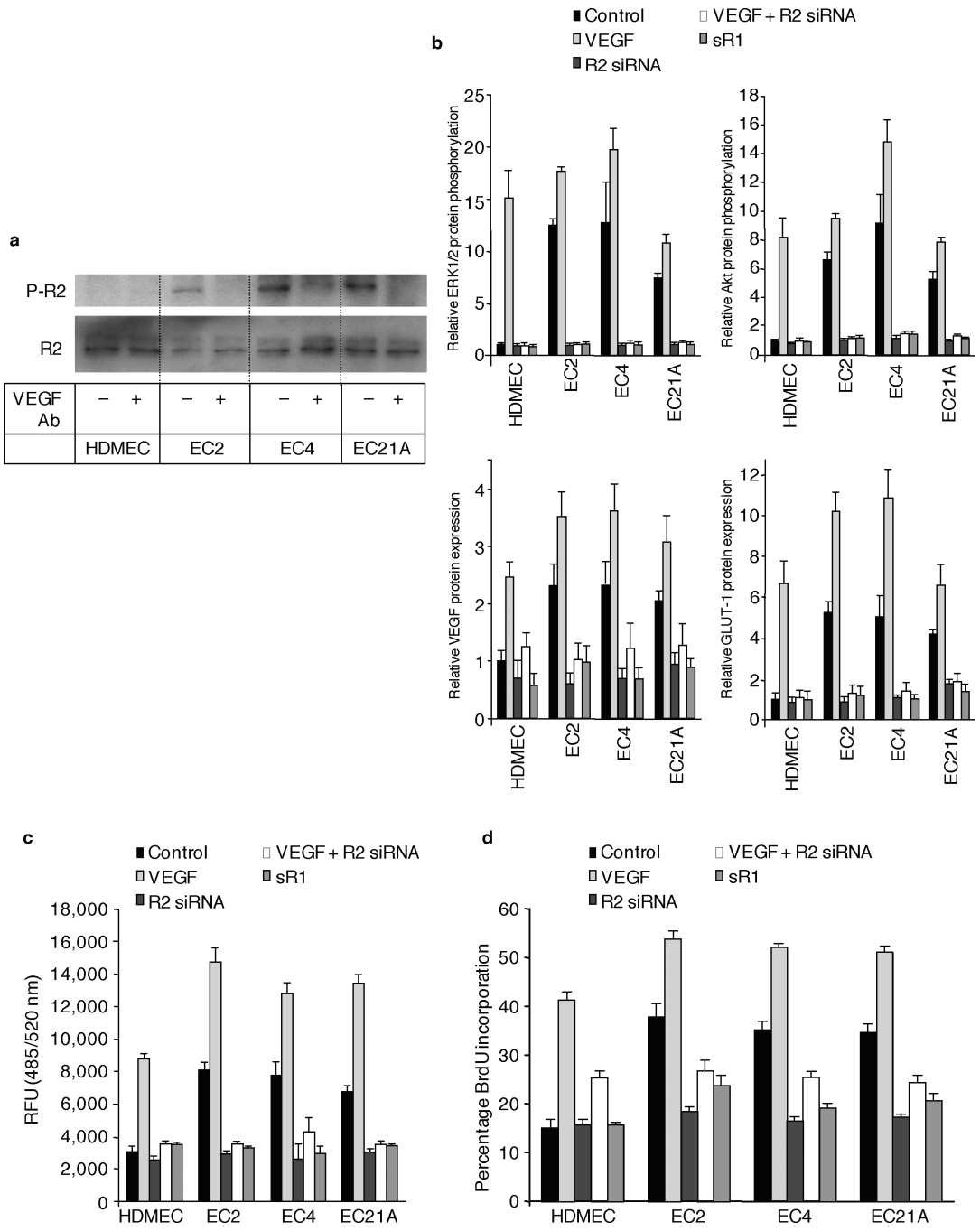

Fig. 1. VEGFR2-dependent signal transduction is upregulated in hemEC

(**a**) Immunoblotting of lysates with antibodies against phospho-VEGFR2 Tyr1175 (P-R2) and VEGFR2 (R2). After overnight serum-starvation, HDMEC and hemEC were pretreated with 2 μg ml^{-1} VEGF neutralizing antibody (VEGF Ab; + lanes) or isotype control mouse IgG (− lanes) for 48 hours.

(**b**) Normalized results of quantitative multiplex ELISA for several targets of VEGFR2 signaling. Data were normalized by dividing experimental values by α-tubulin values. HDMEC and three different hemEC were treated with either control siRNA (black, light

gray and medium gray bars) or *VEGFR2*-specific siRNA (R2 siRNA) (dark gray and white bars). Also, cells were treated with vehicle (PBS + 0.1% BSA, black bars) or 25 ng ml^{-1} VEGF for 15 min (light gray bars, to measure protein phosphorylation) or 12 h (light gray bars, to measure protein expression). Finally, the effect of adding 50 ng ml^{-1} recombinant sVEGFR1 (sR1) was tested (medium gray bars). Control experiments showed that levels of *VEGFR2* transcripts were reduced by > 80% in cells treated with *VEGFR2* siRNA (not shown). Error bars represent SD +1 (n = 3).

(**c**) Increased cell migration of hemEC compared to HDMEC. Cells were treated as described in Fig. 1b. Data expressed as relative fluorescence units (RFU). Error bars represent SD of +1 (n = 3).

(**d**) Increased proliferation of hemEC without exogenous VEGF by FACS analyses of BrdU incorporation. Cells were treated as described in Fig. 1b. Numbers indicate the percentage of BrdU positive cells. Error bars represent SD of +1 (n = 3).

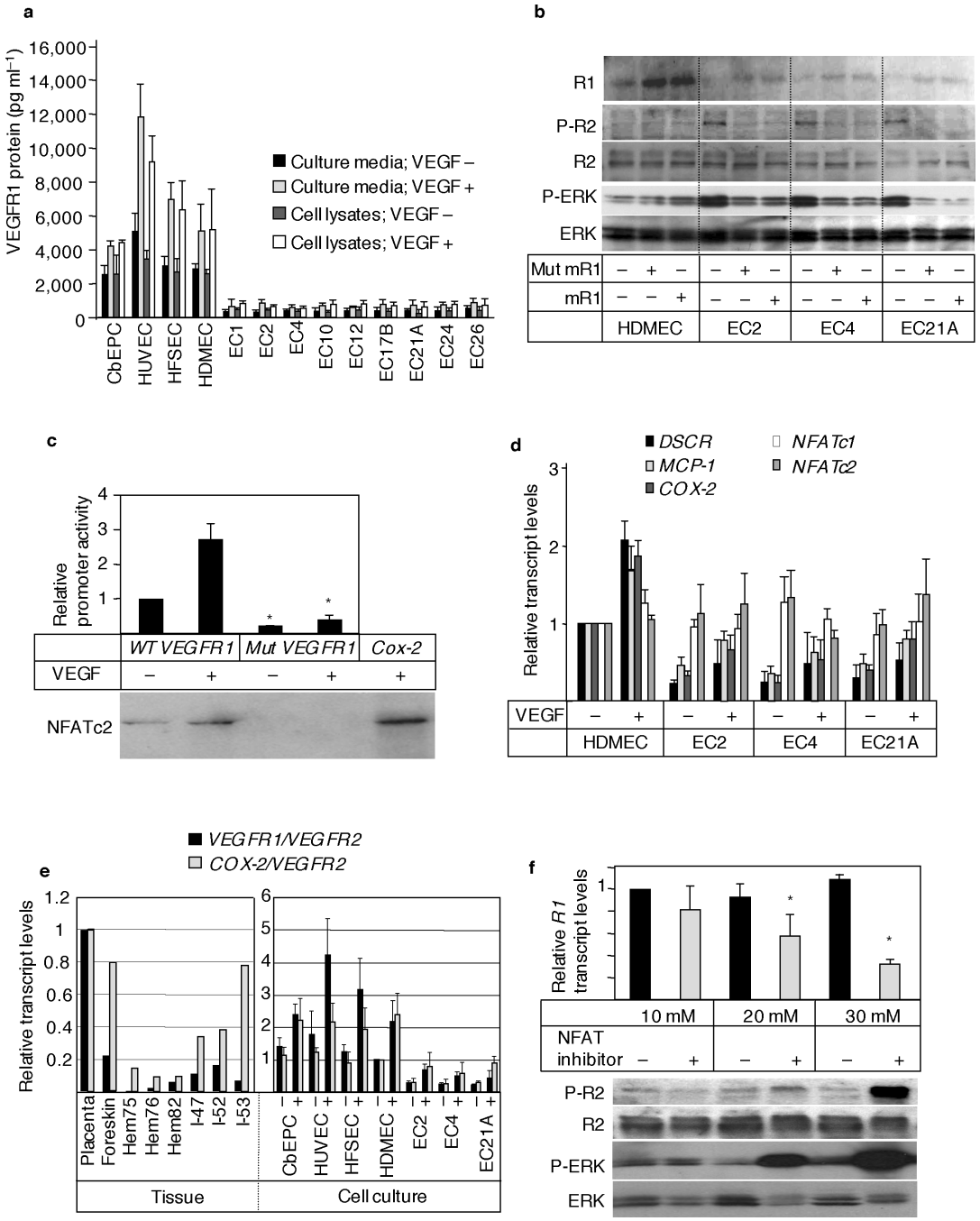

Fig. 2. Low level VEGFR1 expression in hemEC caused by reduced activation of NFAT

(**a**) Mean concentrations of VEGFR1 protein by ELISA in culture media (for measuring sVEGFR1) and cell lysates (for measuring total VEGFR1) of control cells (cbEPC, HUVEC, HFSEC, HDMEC) and nine different hemEC. Cells were incubated in serum-free medium for 24 h in the absence (−) or presence (+) of 25 ng ml^{-1} VEGF. For all hemEC, the levels of VEGFR1 protein were significantly lower ($P < 0.05$) than the value for unstimulated HDMEC. Error bars represent SD of +1 ($n = 3$).

(**b**) Effects of retroviral overexpression of full-length membrane-bound form of VEGFR1 (mR1; + lanes) or Y1213F mutated VEGFR1 (Mut mR1) on levels of VEGFR2 (R2) and ERK and their phosphorylated forms (P-R2 and P-ERK) in HDMEC and hemEC. Control cells were transfected with empty vector. VEGFR1 expression was detected using antibody to VEGFR1.

(**c**) NFAT is a transcriptional activator of the *VEGFR1* promoter.

Top: The difference in relative *VEGFR1* promoter activity in HDMEC when transiently transfected with wild-type (WT) or mutated (Mut) *VEGFR1* promoter-luciferase construct, and when incubated without (−) or with (+) VEGF for 3 h. Luciferase activity in HDMEC with wild-type *VEGFR1* and without VEGF set at 1. Data are expressed as means of three independent experiments. *$P < 0.05$ as compared with the value for cells transfected with wild-type *VEGFR1* promoter construct; error bars represent SD of +1 ($n = 3$).

Bottom: DNA binding activity of NFAT to biotin-labeled *VEGFR1*- or control *COX-2* promoter oligonucleotides. An oligonucleotide representing the promoter of *COX-2*, a known NFAT target gene, used as a positive control. Cell lysates from HDMEC incubated without (−) or with (+) VEGF for 15 min were used.

(**d**) Real-time quantitative PCR used to measure *DSCR1*, *MCP-1*, *COX-2*, *NFATc1* and *NFATc2* transcripts in lysates of HDMEC and hemEC incubated in the absence (−) or presence (+) of 25 ng ml^{-1} of VEGF for 6 h. Transcript levels were normalized to *GAPDH*. Levels in HDMEC without VEGF were set at 1. For hemEC, the levels of *DSCR1*, *MCP-1* and *COX-2* mRNA were significantly lower ($P < 0.05$) than the value for HDMEC. Error bars represent SD of +1 ($n = 3$).

(**e**) Relative transcript levels (to *VEGFR2*) of the NFAT target genes, *VEGFR1* and *COX-2*, in control tissues (placenta, foreskin), hemangioma tissues, control cells (cbEPC, HUVEC, HFSEC, HDMEC) and hemEC using real-time quantitative PCR. Hemangioma tissues consisted of 3 proliferating phase hemangiomas (hem75, hem76, and hem82) and 3 involuting hemangiomas (I-39, I-47 and I-52) (see also48). Cultured cells were incubated without (−) or with (+) VEGF (25 ng ml^{-1}) for 6 hours. To allow comparisons to be made between the tissues and the cultured endothelial cells, we chose to compare the *VEGFR1* and *COX-2* transcript levels relative to *VEGFR2* (assuming the two VEGF receptors are endothelial cell-specific48). The *VEGFR1/VEGFR2* or *COX-2/VEGFR2* transcript ratios for placenta and HDMEC without VEGF were set at 1. No significant differences between *VEGFR2* transcript levels (relative to *GAPDH*) in HDMEC and hemEC were found (not shown).

(**f**) Treatment with cell-permeable selective NFAT inhibitor downregulates VEGFR1 expression and induces phosphorylation of VEGFR2 and the downstream target ERK.

Top: Relative amounts of *VEGFR1* (*R1*) transcripts determined by real-time quantitative PCR in lysates of cells not treated (−; black bars) or treated (+; light gray bars) with the cell-permeable NFAT inhibitor III (INCA-6; Calbiochem). HDMEC were treated with 10−30 μM inhibitor for 12 h. Value for lysates of untreated cells in the experiment with 10 μM INCA-6 was set at 1. * $P < 0.05$ as compared with the value in cells without inhibitor; error bars represent SD of +1 ($n = 3$). *Bottom*: Immunoblotting performed as described in Fig. 1a of cell lysates incubated with indicated concentrations of INCA-6.

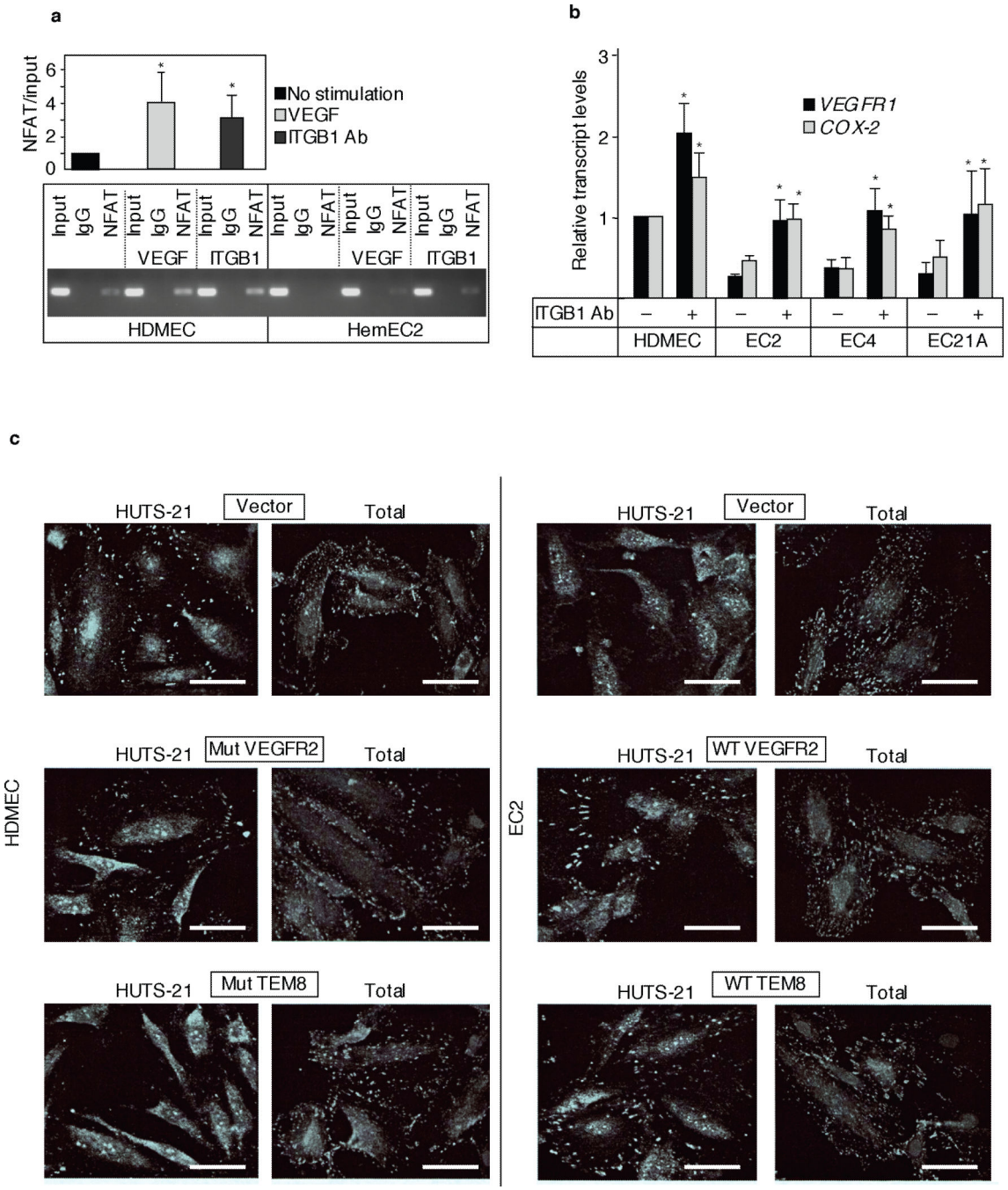

Fig. 3. Reduced activation of β1 integrin in hemEC

(**a**) *In vivo* interaction of NFATc2 with *VEGFR1* promoter assayed by chromatin immunoprecipitation.

Top: HDMEC were stimulated with (+) or without (−) VEGF (25 ng ml^{-1}), β1 integrin stimulating antibody (ITGB1 Ab, 10 μg ml^{-1}) or control IgG for 30 min and the amount of *VEGFR1* promoter fragments in the precipitate was quantitated using real-time PCR as described in Supplementary Methods. * $P < 0.05$ as compared with the value in unstimulated cells; error bar represents SD+1 ($n = 3$).

Bottom: In HDMEC and hemEC2, the presence of *VEGFR1* promoter fragments in the precipitates was detected using PCR followed by agarose gel electrophoresis. Similar results were obtained with hemEC4 and hemEC21A.

(**b**) Real-time quantitative PCR was used to measure *VEGFR1* (black bars) and *COX-2* (light gray bars) transcripts in lysates of HDMEC and hemEC incubated in the absence (−) or presence (+) of 10 μg ml^{-1} β1 integrin antibody (ITGB1 Ab; + lanes) for 6 h. Transcript levels were normalized to *GAPDH*. Levels in HDMEC without the antibody were set at 1. **P* < 0.05 by Mann-Whitney test; error bars represent SD of +1 (*n* = 3).

(**c**) Immunocytochemical detection of active (HUTS-21) and total β1 integrin (total) on cell surface of HDMEC (left) transfected with vector, mutant VEGFR2 (Mut VEGFR2) or mutant TEM8 (Mut TEM8), compared with $hemEC2^{(VEGFR2)}$ (right) transfected with vector, wild-type VEGFR2 (WT VRGFR2) or wild-type TEM8 (WT TEM8). Similar results were obtained with $hemEC4^{(TEM8)}$ and hemEC21A. White scale bars are 50 μm.

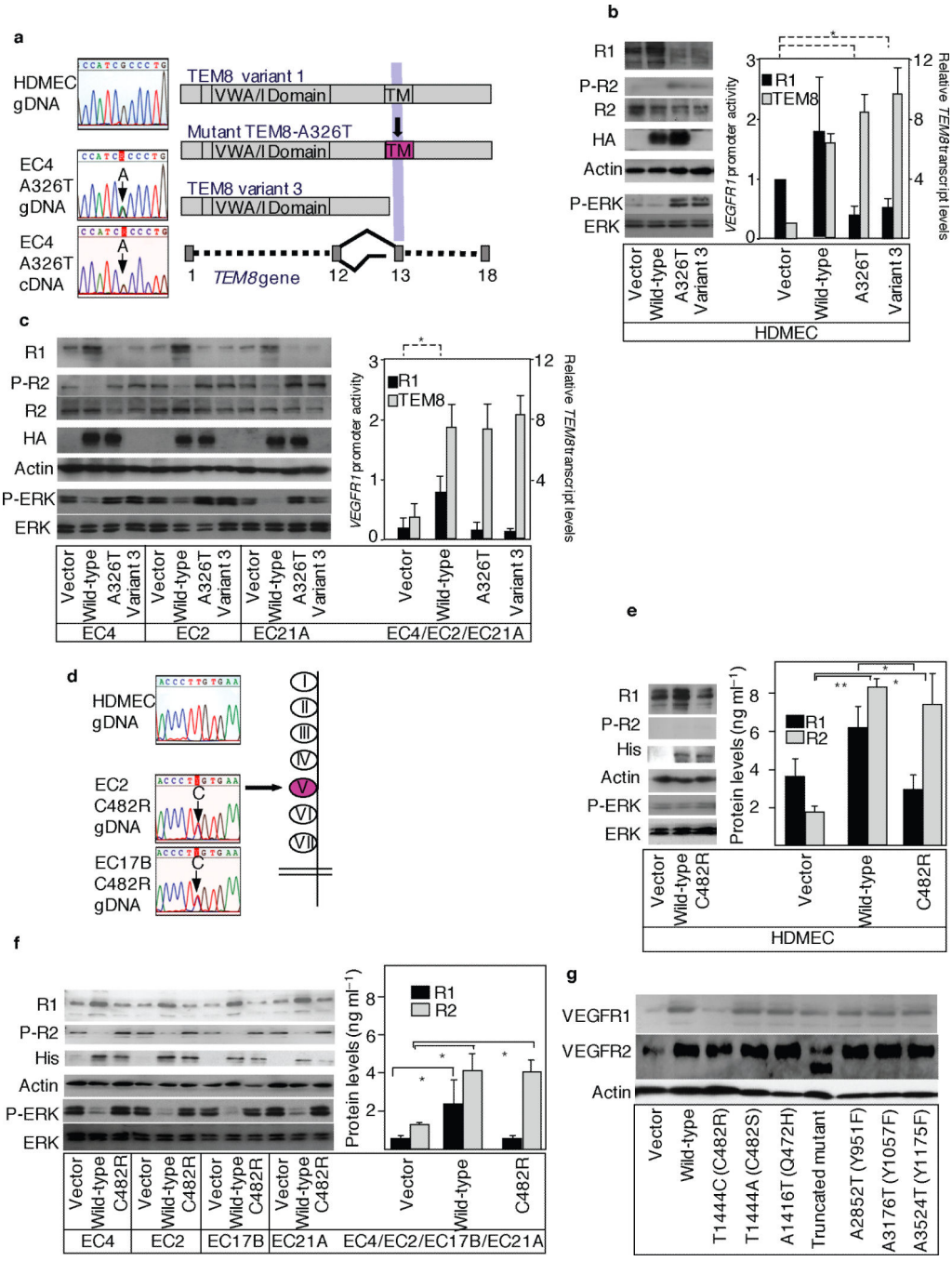

Fig. 4. TEM8 and VEGFR2 mutations and their effects

(**a**) Left: Portions of nucleotide sequence tracings of genomic DNA from HDMEC (control) and genomic DNA and cDNA from cells of hemangioma patient 4 show heterozygosity for G and A (arrows) in *TEM8* in hemEC4.

Right: Diagrams illustrating the domain structure of wild-type TEM8 protein variant 1 (top), mutant TEM8-A326T and TEM8 variant 3. Selected exons (1, 12, 13 and 18) within the *TEM8* gene are shown (bottom). *Variant 1* transcript is generated by splicing exon 12 to

exon 13; *variant 3* transcript is generated by splicing exon 12 to a cryptic exon within intron 12 and terminates upstream of exon 13.

(**b**) Left: The effects of overexpressing constructs coding for TEM8 in HDMEC. Lysates from cells transfected with vector or constructs encoding HA-tagged wild-type TEM8, HA-tagged A326T mutant TEM8 or variant 3 were used for immunoblotting with antibodies against VEGFR1 (R1), phospho-VEGFR2 Tyr1175 (P-R2), VEGFR2 (R2), HA-tag (HA), actin, phospho-ERK (P-ERK) and ERK. Transfection efficiency was determined by GFP expression (> 95%).

Right: Quantitation of *VEGFR1* and *TEM8* expression. To determine *VEGFR1* promoter activity, *VEGFR1* promoter-luciferase reporter was transfected into HDMEC transfected with retroviral constructs described in **Fig. 4b** left (black bars). *TEM8* expression was measured by real-time PCR (light gray bars). The bar graph shows fold stimulation, with the value in HDMEC transfected with retroviral vector arbitrarily set at 1. * $P < 0.05$ as compared with the value in cells transfected with retroviral vector. Error bars represent SD +1 ($n = 3$). The changes in *VEGFR1* promoter activity correlate with changes in VEGFR1 protein expression.

(**c**) Left: Immunoblotting of lysates prepared from hemEC4$^{(TEM8)}$, hemEC2$^{(VEGFR2)}$ and hemEC21A transfected with retroviral constructs as described in Fig. 4b.

Right: Quantitative assay of *VEGFR1* and *TEM8* expression as described in **Fig. 4b**. For this assay, a mixture of equal amounts hemEC2$^{(VEGFR2)}$, hemEC4$^{(TEM8)}$ and hemEC21A lysates was used. The bar graph shows levels of *VEGFR1* promoter activity (black bars) and *TEM8* transcript levels (light gray bars), relative to the value in HDMEC transfected with retroviral vector arbitrarily set at 1 in **Fig. 4b**. *$P < 0.05$ as compared with the value in cells transfected with retroviral vector. Error bars represent SD+1 ($n = 3$). The changes in *VEGFR1* promoter activity correlate with changes in VEGFR1 protein expression.

(**d**) Portions of nucleotide sequence tracings of genomic DNA from cells of control individuals (HDMEC) and cells (hemEC) from hemangioma patients 2 and 17 demonstrate heterozygosity for T and C (arrows) in *VEGFR2* in hemEC. Sequencing of blood-derived DNA demonstrated heterozygosity for T and C alleles in both patients. The T-to-C transition results in a substitution of Cys482 by arginine in the Ig-like domain V (arrow) in the extracellular domain of VEGFR2 (at right).

(**e**) Left: The effects of overexpressing constructs coding for VEGFR2 in HDMEC. Following retroviral transfer of expression constructs into HDMEC, lysates from cells transfected with vector or constructs encoding His-tagged wild-type VEGFR2 or His-tagged mutant VEGFR2 were subjected to immunoblotting with antibodies to VEGFR1 (R1), phospho-VEGFR2 Tyr1175 (P-R2), His-tag (His), actin, phospho-ERK (P-ERK) and ERK. Transfection efficiency was determined by GFP expression (> 95%).

Right: VEGFR1 (black bars) and VEGFR2 (light gray bars) protein concentrations determined by ELISA in lysates of HDMEC transfected with retroviral vector, or constructs encoding wild-type or mutant VEGFR2. *$P < 0.05$, **$P < 0.01$ as compared with the value for cells transfected with vector. Error bars represent SD of +1 ($n = 3$).

(**f**) Left: Immunoblotting of lysates prepared from hemEC4$^{(TEM8)}$, hemEC2$^{(VEGFR2)}$, hemEC17B$^{(VEGFR2)}$ and hemEC21A transfected with retroviral constructs.

Right: Quantitative ELISA of VEGFR1 (black bars) and VEGFR2 (light gray bars). Protein levels were determined in a mixture of equal amounts of lysates from hemEC2$^{(VEGFR2)}$,

hemEC4$^{(TEM8)}$ and hemEC17B$^{(VEGFR2)}$ and hemEC21A, stably transfected with retroviral constructs as described in **Fig. 4e**. *$P < 0.05$ as compared with the value for cells transfected with retroviral vector. Error bars represent SD+1 ($n = 3$).

(**g**) Immunoblots of lysates of hemEC2$^{(VEGFR2)}$ overexpressing wild-type or mutant forms of VEGFR2 probed with antibodies against VEGFR1 (R1), VEGFR2 (R2) and actin. Constructs, stably transfected into cells using retrovirus, included empty vector and constructs encoding wild-type VEGFR2, the T1444C/C482R mutation, T1444A/C482S, A1416T/Q472H, VEGFR2 lacking the cytoplasmic domain, A2852T/Y951F, A3176T/Y1057F, and A3524T/Y1175F. A Q472H substitution, reported as a potential hemangioma mutation4, did not affect VEGFR2 stimulation of VEGFR1 expression. This is consistent with the finding that the Q472H *VEGFR2* allele is common (about 50%) among “control” chromosomes. Similar results were obtained with hemEC4$^{(TEM8)}$ and hemEC21A.

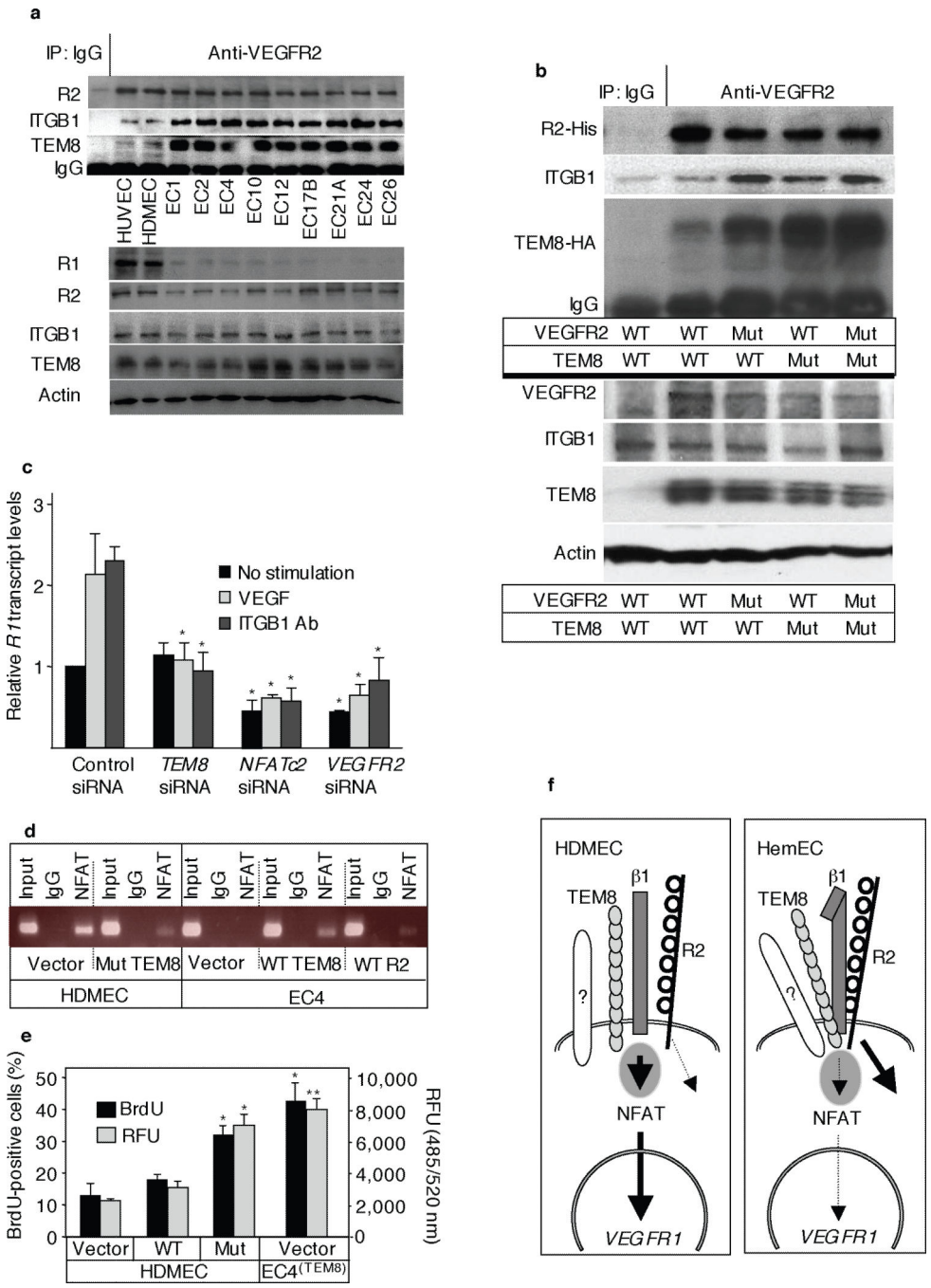

Fig. 5. Integrin/VEGFR2/TEM8- and NFAT-mediated stimulation of VEGFR1 expression is repressed in hemangioma endothelial cells

(**a**) Top: Immunoblotting of cell lysates from control cells (HUVEC, HDMEC) and all nine hemEC subjected to immunoprecipitation (IP) with anti-VEGFR2 antibodies or control IgG. The blot was incubated with antibodies to VEGFR2 (R2), β1 integrin (ITGB1) and TEM8. Bottom: The expression levels of VEGFR1, VEGFR2, β1 integrin and TEM8 in HDMEC and hemEC. Immunoblotting was performed with whole cell lysates using antibodies to VEGFR1, VEGFR2, β1 integrin or TEM8. The levels of actin are shown as loading controls.

(**b**) Top: Immunoblotting of lysates from 293-EBNA cells subjected to immunoprecipitation (IP) with antibody to VEGFR2 or control IgG. Cells were stably transfected with combinations of constructs encoding wild-type (WT) and mutant (Mut) VEGFR2 (His-tagged and puromycin-resistant) and TEM8 (HA-tagged and hygromycin B-resistant). Transfected cells were selected for both puromycin (10 μg ml^{-1}) and hygromycin B (300 μg ml^{-1}) resistance. Gel electrophoresis followed by immunoblotting with antibody to β1 integrin (ITGB1), His-tag (R2-His) and HA-tag (TEM8-HA).
Bottom: The expression levels of β1 integrin, TEM8 and VEGFR2 in 293 cells transfected with constructs encoding VEGFR2 and TEM8 as described in **Fig. 5b** Top. Immunoblotting was performed with whole cell lysates using antibodies to VEGFR2, β1 integrin or TEM8. The levels of actin are shown as loading controls.
(**c**) Stimulation of *VEGFR1* transcript levels by VEGF or β1 integrin stimulating antibodies (ITGB1 Ab) in HDMECs requires TEM8, NFATc2 and VEGFR2. Cells were treated with specific siRNAs or control siRNA and cultured without (black bars) or with VEGF (light gray bars) or β1 integrin antibody (dark gray bars) for 6 h. Control experiments showed transcript levels for each siRNA target gene to be reduced by > 80% (not shown). Relative amounts of *VEGFR1* transcripts (normalized with GAPDH) determined in total RNA with quantitative PCR. Error bars represent SD of +1 ($n = 3$). * $P < 0.05$ as compared with the values in control cells.
(**d**) *In vivo* interaction of NFATc2 with *VEGFR1* promoter assayed by chromatin immunoprecipitation. HDMEC and $hemEC4^{(TEM8)}$ were transfected with retroviral vector or constructs encoding mutant TEM8 (Mut TEM8) , wild-type TEM8 (WT TEM8) or wild-type VEGFR2 (WT R2). The presence of *VEGFR1* promoter fragments in the precipitates was detected using PCR followed by agarose gel electrophoresis. Transfection efficiency was determined by GFP expression (> 95%). Similar results were obtained with $hemEC2^{(VEGFR2)}$ and hemEC21A.
(**e**) Increased proliferation and migration of HDMEC following stable transfection with construct encoding mutant TEM8. HDMEC were stably transfected with retroviral vector or constructs encoding wild-type (WT) TEM8 or mutant (Mut) TEM8. $HemEC4^{(TEM8)}$ cells with empty vector were included for comparison. For proliferation analysis, cells were labeled with BrdU and analyzed by flow cytometry. Bar heights represent proportions of BrdU-positive cells. For migration analysis, cells were assayed as described in Fig. 1d. *$P < 0.05$; **$P < 0.01$ comparing proliferation or migration to vector control. Error bars represent SD+1 ($n = 3$).
(**f**) Diagram summarizing pathways that are affected in hemangioma. In control endothelial cells, such as HDMEC (left), activation of NFAT and VEGFR1 (R1) expression is controlled by a functional interaction between integrin, the VEGFR2 extracellular domain and TEM8. This results in high levels of VEGFR1 (and COX-2, DSCR-1) and low levels of VEGF-dependent VEGFR2 signaling. In hemEC (right), repressed NFAT activation causes low expression of VEGFR1 (and COX-2, DSCR-1). This results in high level VEGF-mediated signaling through activation of VEGFR2-tyrosine kinase. Consequently, proliferation and migration are upregulated. The effects of mutations in TEM8 and VEGFR2 on VEGFR2 phosphorylation and downstream pathways are indirect and linked to downregulated activation of integrin-NFAT and low VEGFR1 expression. In $hemEC4^{(TEM8)}$, mutant TEM8 has a dominant negative effect on the integrin-NFAT-

VEGFR1 pathway. In patient 4 this provides a sufficient genetic explanation for the hemangioma signaling phenotype. The C482R mutation in hemEC2$^{(VEGFR2)}$/17B$^{(VEGFR2)}$ represents a loss-of-function mutation in the context of VEGFR1 expression, but it does not appear to be sufficient to induce a hemEC-like phenotype when overexpressed in HDMEC. There are two possible reasons; one possibility is that viral expression of mutant VEGFR2 does not reach the required level (in hemEC2 and 17B the ratio between wild-type and mutant protein is 1:1, but this ratio may need to be even more in favor of the mutant in a cell that already expresses two wild-type alleles); a second possibility is that the VEGFR2 mutation is associated with an additional genetic or physiological change to generate the hemangioma cellular phenotype of repressed integrin-NFAT activity and low VEGFR1 expression. In hemEC from patients where we have not yet found mutations, we speculate that their increased β1 integrin/VEGFR2/TEM8 complex formation and reduced integrin/NFAT/VEGFR1 activity is associated with mutations in other, as yet unidentified, cell surface (stippled bars) or cytoplasmic (grey areas with arrows) components of the pathway.

Table 1

Protein phosphorylation levels in hemEC compared to HDMEC

Probe	HDMEC + VEGF	EC2	EC4	EC21A
VEGFR2 (Y951)	20.8 ± 1.3	11.3 ± 0.9	13.5 ± 4.8	5.7 ± 1.1
VEGFR2 (Y996)	88.5 ± 41.8	112.8 ± 37.1	98.2 ± 17.1	92.9 ± 36.3
VEGFR2 (Y1054)	36.4 ± 4.3	27.8 ± 2.2	12.9 ± 6.6	3.4 ± 0.6
VEGFR2 (Y1059)	36.3 ± 3.2	27.1 ± 2.2	23.2 ± 7.7	8 ± 0.8
VEGFR2 (Y1175)	16.1 ± 3.6	15.3 ± 1.9	19.3 ± 5.9	24.5 ± 1.4
PLC-γ (Y771)	312.9 ± 25.4	385.3 ± 24.8	226.4 ± 51	40 ± 12.8
RASA1 (Y460)	78.6 ± 14.9	79.7 ± 14.8	69.8 ± 21.3	52.5 ± 19.9
p85A (Y607/S608)	89.7 ± 8	86.9 ± 6.8	58.9 ± 14.2	18.7 ± 1.1
PDK1 (Y9)	213.6 ± 37.9	230.9 ± 48.8	160.1 ± 21.9	91.5 ± 7.5
PDK1 (Y373/Y376)	82.7 ± 14.4	54.5 ± 14.1	65.5 ± 18.4	31 ± 2.4
FAK1 (Y576/Y577)	11 ± 3.8	4.4 ± 1.4	8.2 ± 2.5	6 ± 1
FAK2 (Y579/Y580)	17.7 ± 3	22.2 ± 3.1	15.6 ± 1.4	8.9 ± 1.8
SRC8 (Y499)	20 ± 2.1	19.1 ± 1.9	16.3 ± 0.9	10.5 ± 1.1
Paxillin (Y118)	178.3 ± 41.4	168.1 ± 32.5	198.8 ± 50.2	260.2 ± 84.4
Paxillin (Y31)	34.2 ± 9.4	38.9 ± 10.8	28.4 ± 5.1	14.6 ± 3.7
Vinculin (Y821)	5.9 ± 0.5	6.8 ± 0.7	5.4 ± 2	3.1 ± 0.5
PECAM (Y713)	17.2 ± 1.5	12.8 ± 1.2	14.9 ± 4.8	10.1 ± 5.3
JAK1 (Y1022/Y1023)	32.7 ± 2.2	32.9 ± 1.9	24.2 ± 5.7	28.8 ± 7.2
STAT4 (Y725)	30.1 ± 3.5	21 ± 1.7	18.7 ± 4.4	5.3 ± 0.6
MAPK12 (T183/Y185)	5.4 ± 0.5	26.6 ± 1.7	13.2 ± 6.2	28 ± 18.5
LCK (Y394)	24.2 ± 2.1	37.3 ± 3.2	20.1 ± 9.5	26.4 ± 11.1

Values represent the mean ± SD (n = 3) fold increase compared to HDMEC in the absence of exogenous VEGF.

The differences compared to HDMEC are all statistically significant ($P < 0.05$) by ANOVA.